molecular informatics

DOI: 10.1002/minf.201000131

Docking and Molecular Dynamics Calculations of Pyrrolidinone Analog MMK16 Bound to COX and LOX Enzymes

N. Neophytou,[a, f] G. Leonis,*[b, f] N. Stavrinoudakis,[a] M. Simčič,[c, d] S. Golič Grdadolnik,[c, d] E. Papavassilopoulou,[a] G. Michas,[a] P. Moutevelis-Minakakis,[a] M. G. Papadopoulos,[b] M. Zing,[e] and T. Mavromoustakos*[a]

Presented at the 18th European Symposium on Quantitative Structure Activity Relationships, EuroQSAR 2010, Rhodes, Greece

Abstract: The new molecule 4-[(2S)-2-(1*H*-imidazol-1-yl-methyl)-5-oxotetrahydro-1*H*-pyrrol-1-yl]methylbenzenecarboxylic acid (MMK16) was found to have promising anti-inflammatory activity. This biological behavior of MMK16 triggered our interest to study its binding affinity using NMR spectroscopy in LOX and its docking and molecular dynamics (MD) properties in LOX and COX enzymes. The present NMR and docking binding studies not only rationalize the obtained biological results since in all three receptors MMK16 shows high affinity and scoring but also make it a potential dual LOX-5/COX-2 inhibitor. Thus, this class of molecules must be further investigated for discovering compounds possessing better biological activity and more lasting biological effect.

Keywords: Pyrrolidinone analogs · Drug design · Molecular dynamics · LOX · COX

1 Introduction

Arachidonic acid is liberated from the membrane bilayer due to the enzymatic action of enzyme $cPLA_2$.[1] Arachidonic acid is the precursor of the formation of eicosanoids, lipid mediators that are involved in inflammation and cancer. Cyclooxygenase (COX), the key enzyme in prostaglandin biosynthesis, exists in two distinct isoforms, namely COX-1 and COX-2.[2,3] COX-1 isoform is continuously expressed in most mammalian tissues and is often called "housekeeping" enzyme. COX-2 is induced during inflammatory diseases[4] and it constitutes a potential target to develop new potent anti-inflammatory compounds.[5,6] Arachidonic acid is also the substrate for lipoxygenase-5 (LOX-5), the enzyme that converts arachidonic acid into Leukotriene A_4 (LTA_4)[7]. This is an unstable precursor of cysteinyl leukotrienes LTC4, LTD4, LTE_4 and dihydroxy leukotriene B_4. Leukotrienes are potent eicosanoid lipid mediators with central importance in the process of inflammation, allergic disorders and asthma.[8,9,10] Cyclooxygenase-2 and lipoxygenase-5 are now believed to participate not only in the inflammation responses, but also in the progression of neoplasia.[11,12,13]

Based on the molecular characterization of commercial SARTANs, synthetic peptidic and non-peptidic analogs, a new avenue was explored in an attempt to design and synthesize novel AT_1 antagonists.[14–28] Thus, MMK analogs have been synthesized to possess pyrrolidinone as template instead of biphenyltetrazole segment.[29,30] The lack of significant activity of the synthetic molecules as AT_1 antagonists led us to test them as anti-inflammatory drugs since it is well known from the literature that pyrrolidinone analogs have such a property.[31] Incorporated to their structures is

[a] *N. Neophytou, N. Stavrinoudakis, E. Papavassilopoulou, G. Michas, P. Moutevelis-Minakakis, T. Mavromoustakos*
Kapodistrian University of Athens
Panepistimiopolis, Zographou 15784, Athens, Greece
**e-mail: tmavrom@chem.uoa.gr*

[b] *G. Leonis, M. G. Papadopoulos*
National Hellenic Research Foundation
Institute of Organic and Pharmaceutical Chemistry, Vas. Constantinou 48, 11635 Athens, Greece
**e-mail: gleonis@eie.gr*

[c] *M. Simčič, S. G. Grdadolnik*
Laboratory of Biomolecular Structure, National Institute of Chemistry
Hajdrihova 19, SI-1001 Ljubljana, Slovenia

[d] *M. Simčič, S. G. Grdadolnik*
EN-FIST Centre of Excellence
Dunajska 156, SI-1000 Ljubljana, Slovenia

[e] *M. Zing*
Drug Discovery and Design Center (DDDC)
Box 1201, Shanghai Institute of Materia Medica No. 555 Rd. Zuchongzhi, Shanghai, P. R. China

[f] *N. Neophytou, G. Leonis*
Authors contributed equally to this work

Supporting information for this article is available on the WWW under http://dx.doi.org/10.1002/minf.201000139.

a carboxylate group which is well known to be associated with anti-inflammatory activity. Among MMK analogs, 4-[(2S)-2-(1*H*-imidazol-1-ylmethyl)-5-oxotetrahydro-1*H*-pyrrol-1-yl]methylbenzenecarboxylic acid (MMK16, Figure 1) was found to have the most promising biological properties. The details of its synthesis and biological data will be reported elsewhere.

In the present work, we attempt to rationalize the biological data referring to MMK16 by applying docking and Molecular Dynamics calculations as well as NMR competitive binding studies. Lipoxygenase-3 (LOX-3) was chosen as a candidate target for the following reasons: (a) its unbound 3D crystal structure alone or bound to anti-inflammatory agents has been published; (b) pyrrolidinone analogs are well known to act as anti-inflammatory drugs or to promote anti-inflammatory action; (c) biophysical studies results showed that MMKs have similar thermal effects in lipid bilayers with those of NSAIDS.

Docking studies have been carried out at the active sites of soybean LOX-3, LOX-5, and cyclooxygenase-2 (COX-2), using Surflex-Dock and Glide algorithms. The binding modes of MMK16 at the active site of these enzymes, using Surflex-Dock and Glide were further compared to the binding modes of a known inhibitor of lipoxygenases (caffeic acid at the active site of LOX-3 and LOX-5) and a known inhibitor of COX (aspirin docked at the active site of COX-2). Competitive studies between caffeic acid and MMK16 are also carried out using NMR spectroscopy.

Molecular docking calculations provide useful information regarding the binding patterns within a protein complex, along with a rough estimation of the principal interactions involved. However, due to the lack of a dynamic description of the system, the selection of representative conformations and their corresponding interactions is not feasible. Thus, in order to evaluate the docking results, we have performed molecular dynamics simulations for MMK16 inside COX-2 and LOX-5. Additionally, a more complete understanding of the enzymes' behavior may be gained after the study of dynamic properties such as the flexibility of the systems, dominant hydrogen bonding interactions, conformational changes and hydrophobic environment inside the binding cavities.

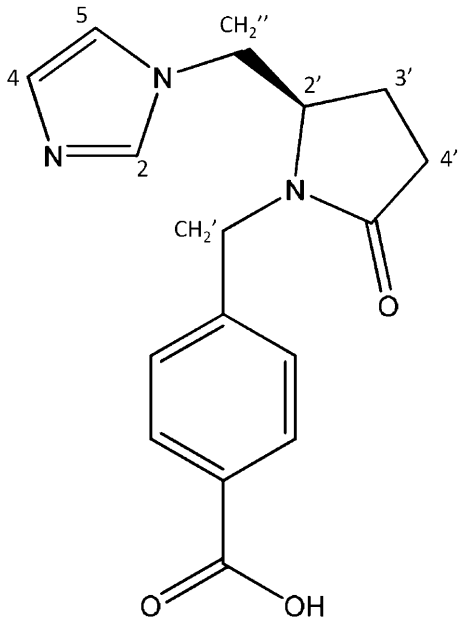

Figure 1. Chemical structure of MMK16.

2 Experimental

2.1 Docking Studies

The structures of the three compounds, caffeic acid, aspirin and MMK16 were constructed using the 2D sketcher module of Sybyl 8.0 molecular modeling interface. The structures were minimized using Tripos Force Field, Steepest Descent, Conjugated Gradient and Powell algorithms (termination: Gradient 0.01 kcal/mol, max iterations: 5000). The conformational space of the compounds, in order to obtain low energy starting conformations, was explored using the Simulated Annealing method.[32,33] The compounds were heated at 2000 K for 2000 fs and annealed at 0 K for 10 000 fs, for 100 cycles. This method resulted in 100 low energy conformations for each compound that were used for docking calculations.

The X-ray crystal structure of soybean lipoxygenase (pdb entry: 1IK3)[34] was obtained from RCSB Protein Data Bank in order to get the detailed insights of the interactions between the enzyme-MMK16 and enzyme-caffeic acid. Prior to docking studies a validation test was performed in order to reproduce the conformation of the co-crystallized ligand 13-HPOD into the active site of soybean lipoxygenase. 13-HPOD[9*Z*,11*E*-13(*S*)-hydroperoxy-9,11-octadecadienoic acid] is a product derived from linolenic acid. The validation tests using Surflex-Dock[35–37] and Glide[38] predicted the binding mode of the ligand at the active site of the enzyme (RMSD 0.65 Å and 0.95 Å respectively, Figure S1).

In order to get the detailed insights of the interactions between the enzyme cyclooxygenase-2 and compounds MMK16 and aspirin, two X-ray crystal structures of the enzyme were used. The X-ray crystal structure of COX-2 co-crystallized with arachidonic acid (pdb entry:1CVU)[39] and the X-ray crystal structure of COX-2 co-crystallized with indomethacin (pdb entry: 4COX).[40] Prior to docking studies, validation tests were performed in order to reproduce the conformation of the co-crystallized ligands for each X-ray crystal structure. The validation tests using Surflex-Dock and Glide predicted the binding mode of ligands arachidonic acid and indomethacin at the active site of the enzyme with pdb entries 1CVU and 4COX, respectively ($RMSD < 1$ Å, Figure S2).

Due to the absence of a crystal structure for lipoxygenase-5, a homology model of the enzyme was used for docking calculations of MMK16 and caffeic acid at the

active site of the enzyme. The homology model of lipoxygenase-5 was kindly provided by Li Du.[41]

The three crystal structures (1IK3, 1CVU, 4COX) and the homology model of lipoxygenase-5 were prepared using the Protein Preparation Wizard utility provided by Schrödinger.[42] According to this utility, bond orders were assigned, crystal water molecules were removed, hydrogen atoms were added, metal Fe(III) of lipoxygenases was treated (this option breaks bonds to metals and adjusts the metal and the neighboring atoms), het states were generated for pH 7.0 for amino acids histidine, glutamic acid and aspartic acid. The 3D structures of proteins were further refined using restraint minimization method for hydrogens only and constraint was set to 0.3 Å (Force field OPLS 2005).

Docking calculations using Surflex-Dock for 1CVU, 4COX and 1IK3 were performed through protomol generation by ligand. The parameters used were threshold 0.5 and bloat 0 for COX-2, and a threshold of 0.3 and bloat 0 were applied to LOX-3. Docking calculations referring to homology model lipoxygenase-5 were performed through protomol generation automatic. Protomol generation parameters were threshold 0.5 and bloat 0. Pre- and post-dock minimizations were performed to provide 5 possible solutions for each annealed conformation.

2.1.1 Docking Calculations Using Glide for 1CVU, 4COX, 1IK3 X-Ray Crystal Structures

Docking calculations were performed using the "Extra Precision" mode of this application. The binding site, for which receptor grid files were generated, was defined by the co-crystallized ligand of each X-ray crystal structure. Dimensions of the enclosing box were 14 Å × 14 Å × 14 Å. "Extra Precision" mode of Glide was also used for docking calculations at the active site of LOX-5. Receptor grid files were generated through definition of active site's amino acids and Fe(III). The size of the enclosing box was 14 Å × 14 Å × 14 Å.

2.2 MD Calculations

After performing molecular docking calculations, MMK16 was initiated from its optimal position (conformation obtained by Glide) to run two MD simulations inside COX-2 (PDB: 1CVU) and LOX-5. An additional simulation was performed for the unbound COX-2. MD simulations have been carried out for the three systems with the SANDER module from the AMBER 11 simulation package.[43,44] The proteins were represented by the modified AMBER ff99SB force field,[45] whereas the ANTECHAMBER module and the general AMBER GAFF force field[46] with AM1-BCC charges[47] were used to obtain the force field parameters for MMK16. For LOX-5, iron was modeled in a +III oxidation state (r_{vdw} = 1.20, ε_{vdw} = 0.05), with no bond restraint between Fe and the ligand. The generalized Born/solvent accessible surface area (GB/SA) implicit solvent model[48] was used (in all simulations) to model the effects of solvation. The SHAKE algorithm[49] was applied to constrain all bond lengths involving hydrogen to their equilibrium distance, and a 2 fs time step was used. The Langevin thermostat with a collision frequency of 3.0 ps^{-1} was used to keep the temperature constant.[50]

The MMK16–protein complex was subjected to 4000 steps of steepest descent minimization, before being used as the initial conformation for a 50 ps MD equilibration. The constant pressure equilibration brought gradually our system from 0 K to 300 K, and no cutoff was used during that time. Finally, the equilibrated conformations were used as the starting point for every subsequent molecular dynamics simulation.

In this study, complex systems containing MMK16 inside COX-2 and LOX-5 as well as unbound COX-2 were simulated for 12 ns each. A cutoff was not used during the simulation, that is, all non-bonded interactions were calculated. For the trajectories obtained, further analysis (hydrogen bonding, distance and Cα atomic fluctuation calculations, solvent-accessible surface area, *RMSD* calculations) was realized with the ptraj module under AMBER.

Solvent-accessible surface area calculations (SASA) calculations were based on the rolling ball algorithm described in reference 51. A value of 1.4 Å was used as a probe radius for the water molecule. SASA values were obtained for MMK16 inside the binding cavity of COX-2 and LOX-5. For the hydrogen bonding calculations we used 3.5 Å as a distance cutoff, along with an angle cutoff of 120°, for all distances and angles, respectively.

2.3 NMR Binding Studies

Samples for NMR STD experiments were prepared in 99.9% D_2O buffer containing 20 mM TRIS (98% D11), 7 mM (ND4)2SO_4 (98% D_8), 3.5 mM $MgCl_2$ and 0.3 mM DTT (98% D10), pD 9. Ligand concentration of 0.4 mM was used and the protein concentration was 0.004 mM. Due to poor solubility of caffeic acid its final concentration in solution was 0.08 mM.

STD NMR experiments[52] were recorded on Varian 800 MHz spectrometer equipped with cold probe with spectral width of 9058 Hz, 8192 complex data points and 10000 scans. Relaxation delay was set to 9 s. Selective on-resonance irradiation frequency was set to 0.32 ppm. Saturation time was initially set to 0.4 s and was then increased to 2 s to obtain better signal to noise ratio in STD spectra. Selective saturation was achieved by a train of 50 ms Gauss-shaped pulses separated by a 1 ms delay. Off-resonance irradiation frequency for the reference spectrum was applied at 30 ppm. Water suppression was achieved with excitation sculpting.[53,54] Spectra were zero filled twice and line broadening function of 1 Hz was applied.

3 Results and Discussion

3.1 Docking Studies of Aspirin and MMK16 at COX-2 Active Site

Aspirin is one of the most widely used non-steroidal, anti-inflammatory drugs worldwide.[31] Aspirin inhibits cyclooxygenase activity through the irreversible formation of a covalent bond with amino acid Ser530. Docking results of aspirin were obtained using the pdb entries 4COX and 1CVU, with Surflex-Dock and Glide. Both algorithms showed identical results and aspirin is localized at the active site in the same way as observed for indomethacin and arachidonic acid.

Figure 2 shows a representative pose of aspirin located in the active site of COX-2 (pdb entry: 1CVU) using Surflex-Dock algorithm.

The orientation of MMK16 in the same pdb entries and using both algorithms was found to be at the same active site. A representative pose using Surflex-Dock is shown in Figure 3. The imidazole ring is positioned at the entrance of the hydrophobic channel (amino acids Tyr355 and

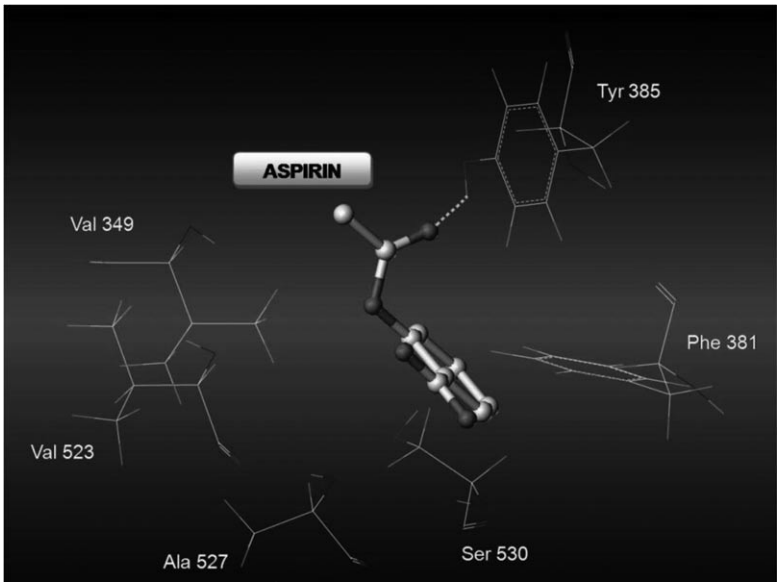

Figure 2. Docking results of aspirin at the active site of COX-2 using Surflex-Dock. The carbonyl group of aspirin forms a hydrogen bond with hydrogen of the phenolic hydroxyl group of the amino acid Tyr385 (O···HO = 2.75 Å, O···O = 3.62 Å).

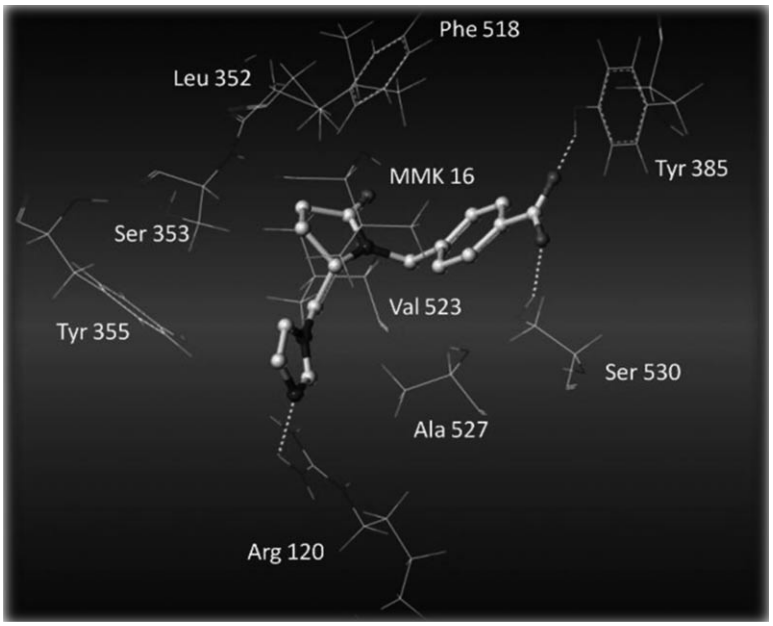

Figure 3. Docking results of MMK16 at the active site of COX-2 (pdb entry:1CVU) using Surflex-Dock.

Arg120) and the carboxylate group is directing towards Tyr385. Three hydrogen bonds (HB) are observed namely, of a nitrogen of imidazole ring with guanidino group of Arg120 (N···HN = 2.62 Å, N···N = 3.31 Å) and the two oxygens of carboxylate group with hydroxyl group of Ser 530 (O···HO = 1.82 Å, O···O = 2.69 Å) and phenolic hydroxyl group of Tyr385 (O···HO = 1.76 Å, O···O = 2.66 Å). MMK16 is further stabilized through van der Waals interactions with the amino acids shown in Figure 3.

3.2 Docking Studies of Caffeic Acid and MMK16 at LOX-3 and LOX-5 Active Site

Docking results of caffeic acid into the active site of soybean LOX-3 (pdb entry 1IK3) using Surflex-Dock and Glide are indicated in Figure 4. The use of both algorithms reveals that the carboxyl group of caffeic acid is positioned towards Fe(III). Surflex-Dock reveals the formation of a hydrogen bond between one phenolic hydroxyl group of caffeic acid and amino acid Gln514 (O···HO = 1.34 Å, O···O = 2.74 Å). In contrast, the results obtained by Glide software reveal the formation of two hydrogen bonds between the two phenolic hydroxyl groups and amino acid Gln514 (O···HO = 2.26 Å, O···O = 3.16 Å and O···HO = 1.76 Å, O···O = 2.70 Å).

Docking studies of MMK16 suggest that the compound is oriented towards the active site of LOX-3 in such a way that the imidazole ring interacts electrostatically with Fe (III). In both algorithms is observed that the compound is also stabilized through van der Waals interactions with the

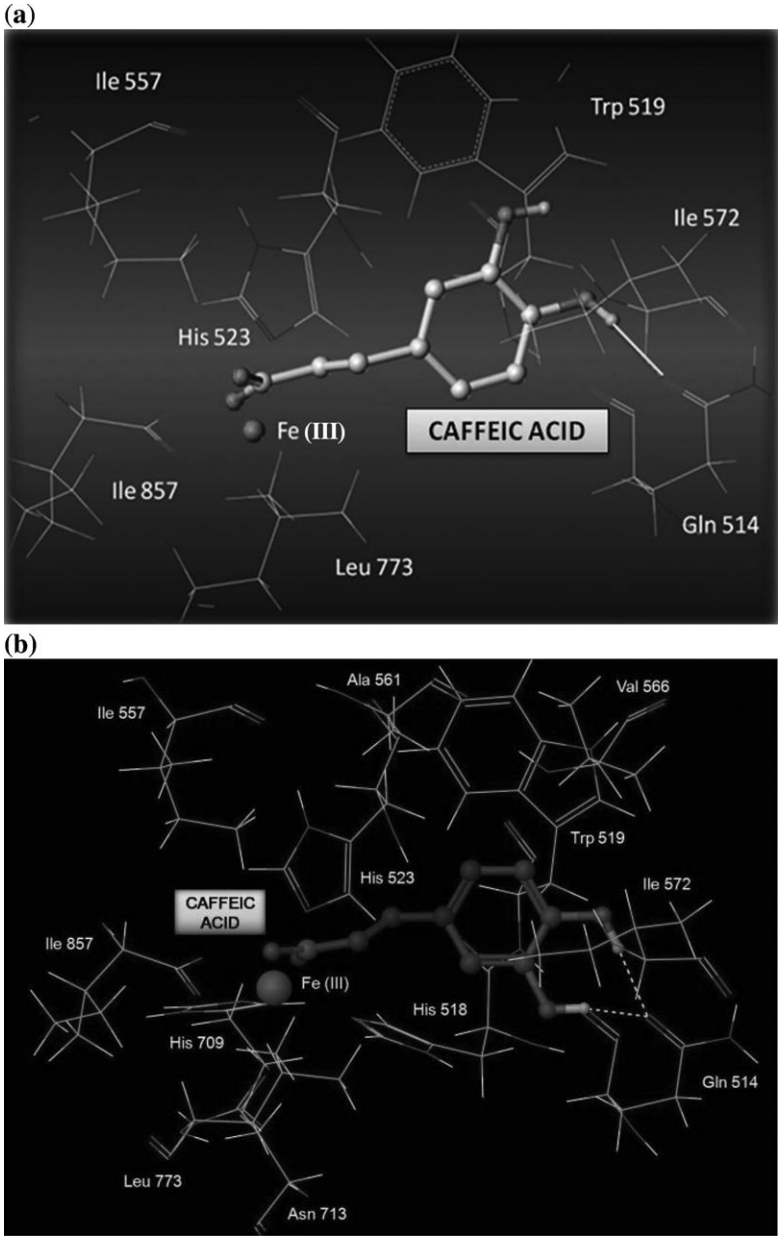

Figure 4. Docking results of caffeic acid at the active site of LOX-3 using a) Surflex-Dock and b) Glide.

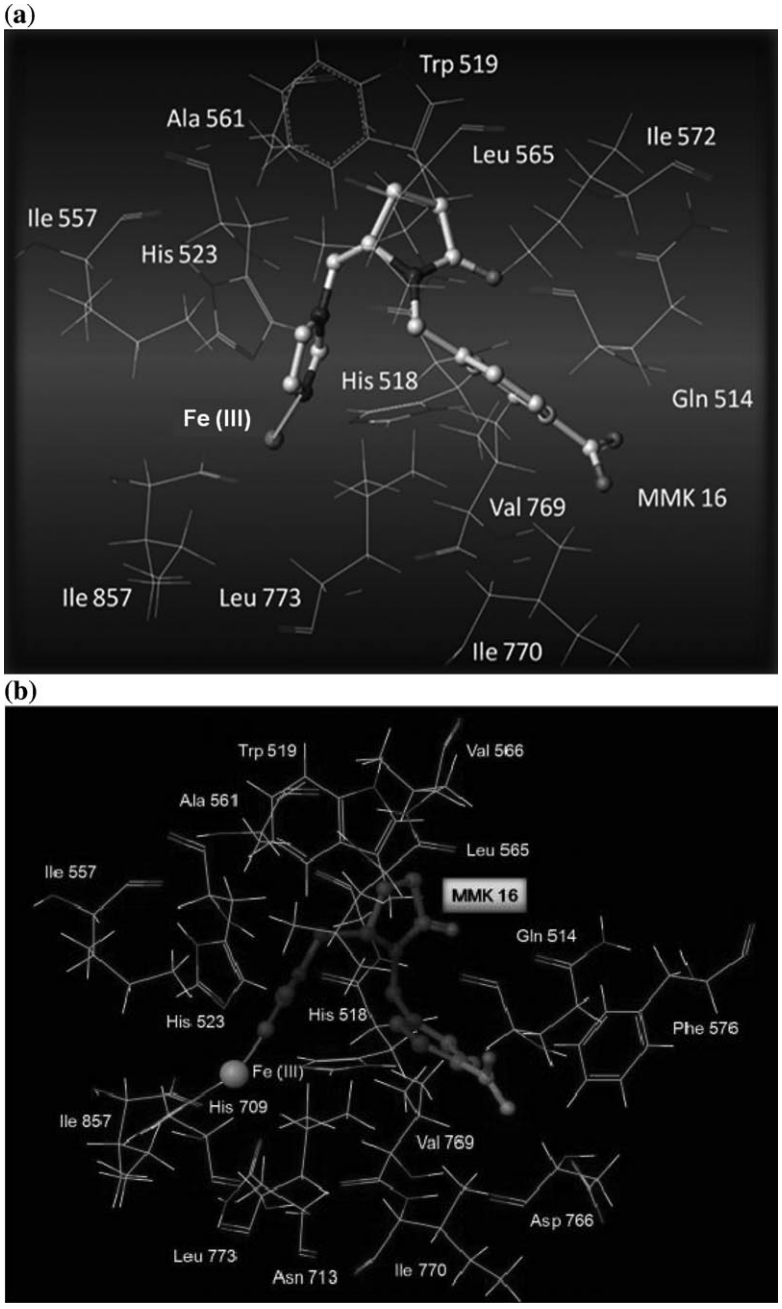

Figure 5. Docking results of MMK16 at LOX-3 using a) Surflex-Dock (N···Fe(III) = 2.35 Å) and b) Glide (N···Fe (III) = 2.63 Å).

amino acids shown as lines in Figure 5. MMK16 is oriented at the active site of LOX-3 in a fashion that the aromatic groups (benzyl and imidazole rings) are stabilized near hydrophobic residues.

Caffeic acid has been also docked into the active site of LOX-5. As shown in Figure 6, both algorithms reveal the same orientation of the compound at the active site. The results only differ on the number of hydrogen bonds. Surflex-Dock proposes a hydrogen bond network between the phenolic hydroxyl groups of caffeic acid and amino acids Gln364 (O···HN = 2.67 Å, O···N = 2.70 Å, and O···HN = 2.11 Å, O···N = 2.17 Å for one hydroxyl group. For the second hydroxyl group the distances are O···HN = 2.17 Å and O···N = 3.18 Å) and Gln558 (O···HN = 1.64 Å and O···N = 2.84 Å). The oxygens of the carboxylate group form two hydrogen bonds with amino acid Asn408 (O···HN = 1.98 Å, O···N = 2.95 Å and O···HN = 2.63 Å, O···N = 3.06 Å). On the contrary, Glide reveals the formation of a hydrogen bond between a phenolic hydroxyl group and amino acid Asn426 (O···HO = 1.89 Å and O···O = 1.83 Å), and between an oxygen of the carboxylate group and amino acid Gln 558 (O···HN = 2.01 Å and O···O = 1.83 Å).

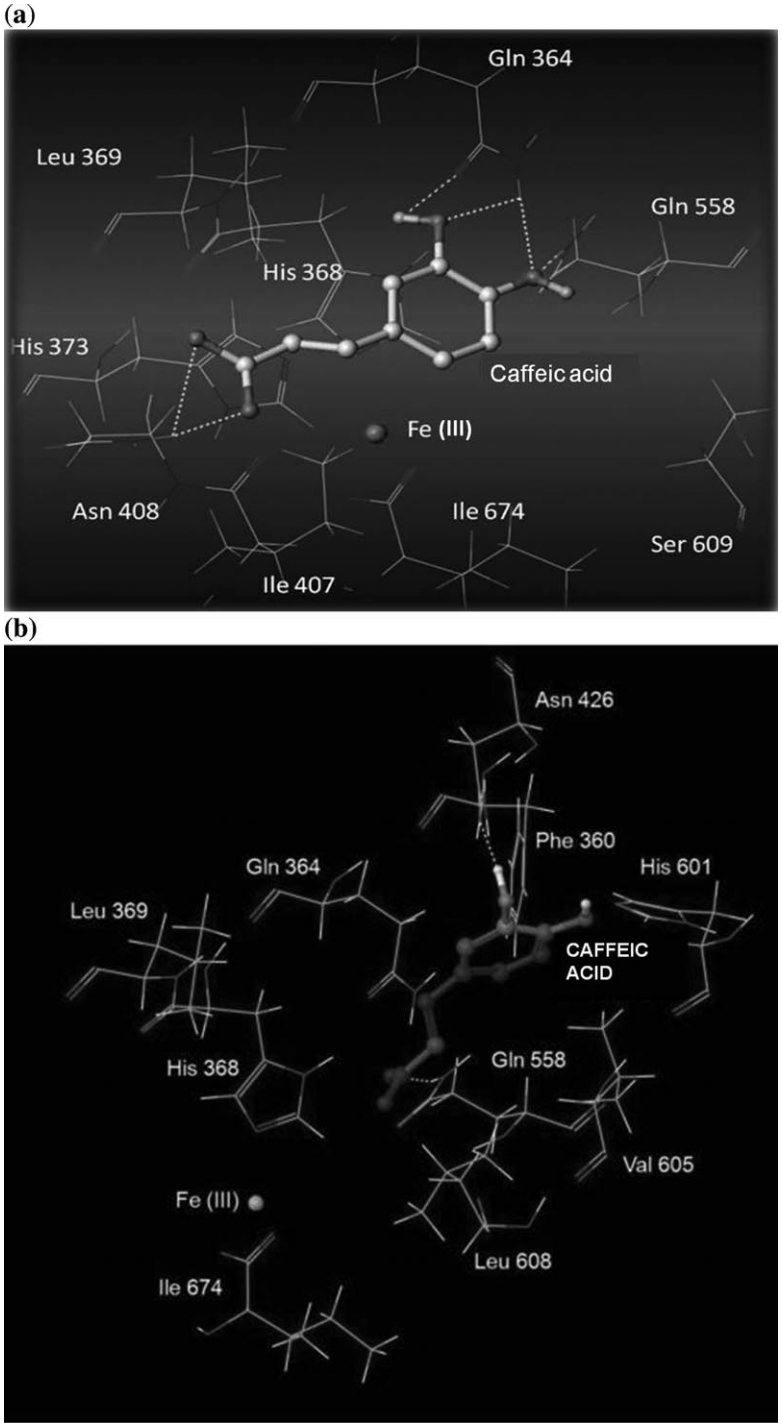

Figure 6. Docking results of caffeic acid at LOX-5 using a) Surflex-Dock b) Glide.

Docking studies of MMK16 at the active site of LOX-5, propose that MMK16 is orienting towards the active site in a manner that electrostatic interaction between imidazole ring and Fe(III) is observed, as depicted in Figure 7. Surflex-Dock results reveal the formation of a hydrogen bond between the oxygen of the pyrrolidinone ring and amino acid Gln364 (O···HN = 2.57 Å and O···N = 3.03 Å) and His433 (O···HN = 2.04 Å and O···N = 2.67 Å), in contrast to Glide that suggests the formation of a hydrogen bond between an oxygen of the carboxylate group and amino acid Asn 426 (O···HN = 2.12 Å and O···N = 2.78 Å).

In Table 1 the binding affinity results are presented as obtained from Surflex-Dock for compounds caffeic acid, aspirin and MMK16. Note that Surflex-Dock score is expressed

Table 1. Comparative scores between MMK16 and the reference compounds aspirin and caffeic acid using XP *G*score and Surflex-dock score values.

	1IK3 XP *G*score	1IK3 $-\log K_d$	LOX–5 XP *G*score	LOX–5 $-\log K_d$	1CVU XP *G*score	4COX XP *G*score	1CVU $-\log K_d$	4COX $-\log K_d$
Caffeic acid	−5.23	3.10	−5.89	3.62	–	–	–	–
MMK16	−6.80	4.15	−5.30	6.40	−9.21	−5.91	7.07	5.16
Aspirin	–	–	–	–	−6.69	−6.40	3.14	3.08

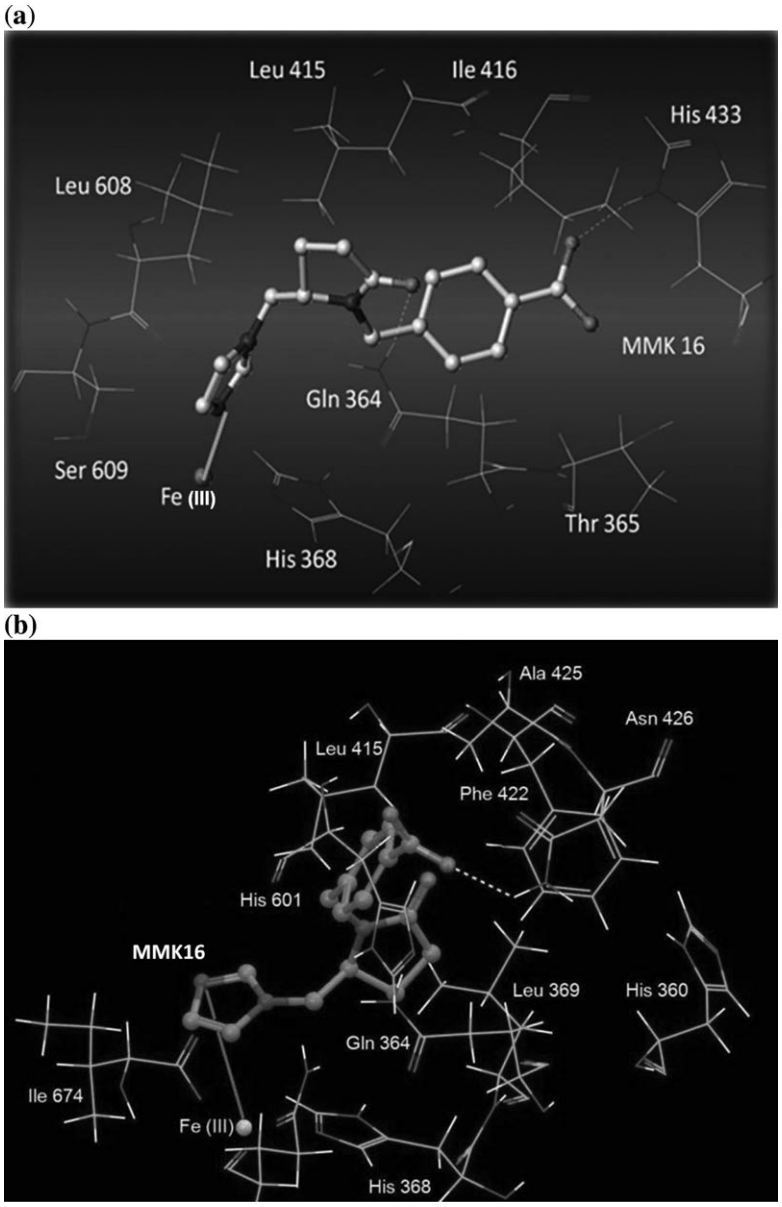

Figure 7. Docking results of MMK16 at the active site of LOX-5 using a) Surflex-Dock (N···Fe(III) = 2.14 Å) and b) Glide (N···Fe(III) = 3.05 Å).

as $-\log K_d$ (K_d refers to dissociation constant). This means that the higher the positive value of the score, the more stable the protein-ligand complex. In terms of XP Gscore, the more negative the value is the more stable is the complex of protein-ligand.

The results of Table 1 show that MMK16 has comparable binding scores with the reference compounds in LOX-3, LOX-5 and COX-2. In most of the cases, these values are even higher, indicating that MMK16 is a molecule that is worth to be biologically evaluated as LOX-5 and COX-2 inhibitor.

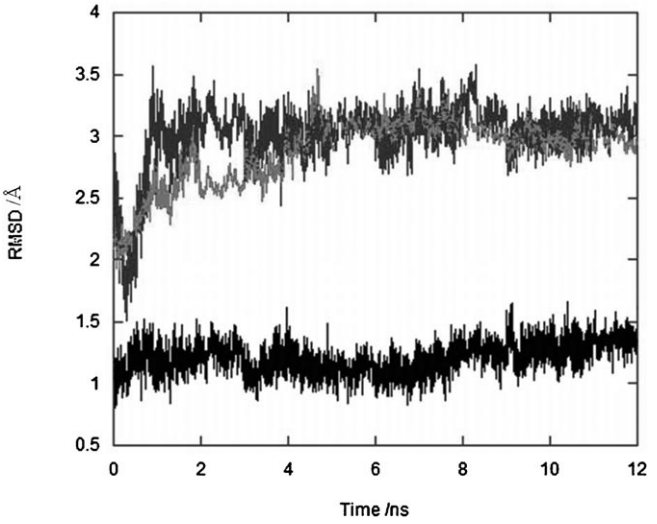

Figure 8. *RMSD* of COX-2 (1CVU) starting from the structure obtained after the Glide calculations and overlapped on the same structure. Superpositions of different backbone atoms are displayed: Cα (light gray), Cα of the membrane-binding domain alone (residues 73–123, dark gray, top), and Cα of active site residues (His90, Arg120, Gln192, Val349, Tyr355, Tyr385, Arg513, Val523, Gly526, Ala527 and Ser530, black, bottom).

3.3 Molecular Dynamics Studies of MMK16 at COX-2 Binding Site

The molecular dynamics simulation of the MMK16–COX-2 complex was initiated from the configuration obtained after the docking calculations (Glide). A noticeable conformational change of the protein in the beginning of the simulation was followed by structural rearrangements during the first 5 ns, and eventually resulted in a relatively stable trajectory. These deviations suggest that the docked structure may not be representative for the system which rather equilibrates towards different conformations. The high degree of stability for COX-2 afterwards, is indicated by the consistency of structural deviations during the simulation (Figure 8, light gray). A Cα-based *RMSD* calculation with respect to the Glide-obtained conformation of COX-2 yielded average values of ≈3 Å, implying that despite the aforementioned conformational changes, the simulation presented moderate fluctuations around a stable average structure. Backbone RMSD for the membrane-binding domain (residues 73–123, Figure 8, dark gray, top) appears equally pronounced, thus suggesting that the complex structure was primarily influenced by changes occurred around this region. It is also observed that some structural changes of the membrane-binding domain (e.g. at 4 ns, and 9 ns) had some impact on the active site (Figure 8, black, bottom). The latter followed a similar pattern (conformational change in the beginning of the simulation), which resulted in a stable structure for the active site region (≈1.4 Å).

Whereas the conformation of COX-2 complex remained relatively stable (after 5 ns), certain regions of the protein presented differences in flexibility. Cα atomic fluctuation calculations for each amino acid of COX-2 revealed that residues such as Glu66, Gln318 and Gly551 appear increasingly flexible, whereas all active site residues belong to the most stable region of the protease with average fluctuations less than 1 Å (Figure S3 and Table S1). In agreement with this observation, the active site in the unbound form of the protein, also appears highly stable (Table S1). This renders the catalytic system as the favorable candidate for sub-

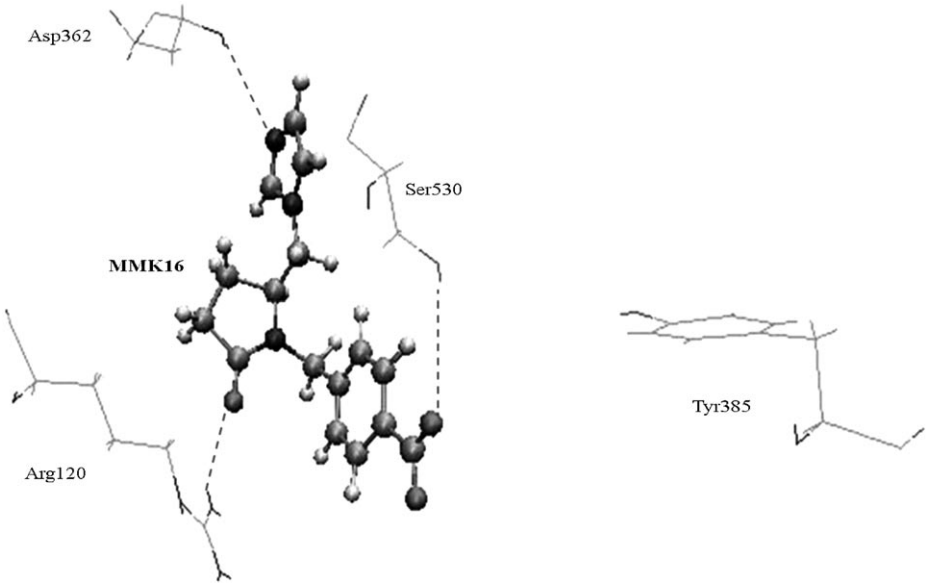

Figure 9. MD results showing hydrogen bonds between MMK16 and active site residues of COX-2. Three principal interactions involving Arg120, Ser530 and Asp362 stabilize MMK16 inside the protein.

strate–protein interactions. The increased flexibility of residues 65–80 (1.5 Å–2.8 Å) may have resulted in the aforementioned structural changes observed for the binding domain (Figure 8, dark gray, top).

Hydrogen bonding analysis on the MD trajectory revealed the reason for the initial instability of the system as observed above. During the course of the simulation, it appeared that the initially observed HB between the imidazole ring of MMK16 and Arg120 has been replaced by a more stable interaction, namely between the pyrrolidinone oxygen of MMK16 and Arg 120, thus resulting in a displacement of MMK16. Consequently, the MMK16 imidazole ring was associated with Asp362 to form another hydrogen bond. This rearrangement also gradually diminished the MMK16–Tyr385 interaction that seized to exist after the first ns. However, the MMK16 carboxylate–Ser530 HB is preserved all through the MD calculations. HB interactions as % occurrence during the simulation are summarized in Table 2, denoting the structural changes induced to the protein: principal HB patterns obtained from the docking calculations may still be present (MMK16–Ser530), while others are unstable (MMK16–Tyr385). A representative binding pose for MMK16 inside COX-2 is illustrated in Figure 9.

Table 2. Principal HB Interactions involving MMK16 and COX-2. O, O1, O2 and N refer to MMK16 atoms. Hydrogen bonds occurring less than 10% of the simulation time are not shown.

Interaction	Occurrence	Comment
Pyrrolidinone O with guanidine Arg120	93%	Appears throughout the simulation
Carboxylate O1 with OH, Ser530	47%	Equally distributed
Imidazole N with amide N, Asp362	25%	Appears mostly after 5 ns
Carboxylate O2 with OH, Ser530	11%	

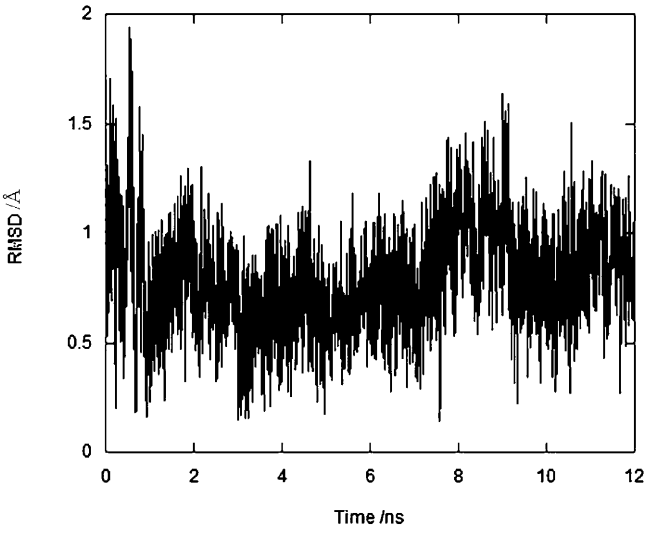

Figure 10. *RMSD* of COX-2 residues Arg120, Asp362, and Tyr385 that participate in unstable HB interactions.

The rearrangement of the hydrogen bonds has obviously contributed to the structural changes observed during our analysis. Considering the *RMS* deviations for Arg120, Asp362 and Tyr385 (Figure 10), we observe that the structural changes associated with HB formation resulted in a conformational rearrangement of the active site. This, along with the structural change of the membrane-binding domain induced an average $\approx$3 Å deviation for the whole protein, eventually leading to a stable, yet altered trajectory.

3.4 Molecular Dynamics Studies of MMK16 at LOX-5 Binding Site

Contrary to COX-2, *RMSD* analysis on the LOX-5 trajectory indicates that a structural change induced to the protein cannot be attributed to conformational changes of the active site (Figure 11). The structure of the protein is stabilized in a new conformation (*RMSD* form initial docked structure $\approx$3.2 Å), while the active site region appears almost identical to the initial conformation with average *RMSD* below 0.5 Å. This combination of events suggests that the change in the conformation of the protein may have resulted by interactions irrelevant to the active site. Furthermore, it could be assumed that the active site residues do not participate in any hydrogen bonds with MMK16, since their conformations remain stable while the overall conformation of the protein has changed. Additionally, Cα atomic fluctuation calculations for the active site residues support this claim, since all fluctuations for residues His368, His373, His551, Asn555 and Ile674 are well below 1 Å.

To further test our docking results we have calculated the distance between the imidazole ring of MMK16 and Fe (III) in the active site (Figure S4). In accordance to the Surflex-Dock results, the Fe-ring distance remains very stable around the average 2.15 Å. Even though Glide provided also a realistic description of the interaction ($\approx$3 Å), it seems overestimated.

Hydrogen bonding analysis for the complex of LOX-5 involves MMK16 in principal interactions with residues Gln364, Asn426 and His601. In agreement with the docking results, a striking observation is that all HB-participating residues are not considered active site residues. Thus, the structural change of the protease may have been induced by a corresponding rearrangement of the hydrogen bonds in another region, without affecting the active site. Surflex-Dock predicted a HB between the pyrrolidinone oxygen of MMK16 and both Gln364 and His433. Although the MD analysis also revealed an interaction between MMK16 and Gln364, it did not yield any results associating His433. Furthermore, it was shown that one of the carboxylate oxygens (instead of pyrrolidinone oxygen) interacts with Gln364. The MMK16 carboxylate O–Asn426 interaction sug-

gested by Glide is also present for half of the simulation, along with a non-predicted MMK16–His601 HB for the second part of the simulation. RMSD calculations for the HB-involved residues Gln364, Asn426 and His601, revealed structures resembling the initial ones with very minor fluctuations ranging from 0.4 Å to 0.8 Å (Figure S5, supporting information). In general, the findings confirm Glide and Surflex-Dock studies (Table 3).

Table 3. Principal HB Interactions involving MMK16 and LOX-5. O1 and O2 refer to the carboxylate oxygen atoms of MMK16. Hydrogen bonds occurring less than 10% of the simulation time are not shown.

Interaction	Occurence	Comment
O1 or O2 with His601	82%	
O1 with Asn426	32%	Appears mostly during the 1st half of the simulation
O1 with Gln364	10%	Appears only in the beginning of the simulation

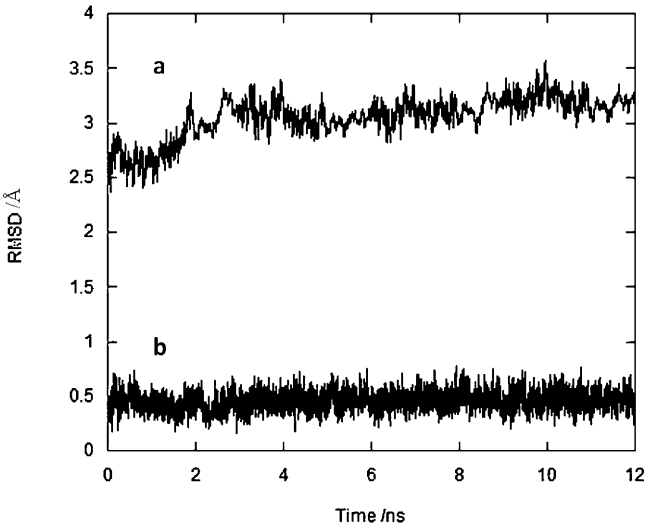

Figure 11. *RMSD* of LOX-5 starting from the structure obtained from the Glide calculations and overlapped on the same structure. Superpositions of different backbone atoms are displayed: a) Cα, and b) Cα of active site residues (His368, His373, His551, Asn555 and Ile674).

Our docking calculations suggest that MMK16 presents higher binding affinity inside COX-2 instead of LOX-5 (see Table 1). This could be partially attributed to the greater number (and the greater appearance frequency) of hydrogen bonds that stabilize MMK16 inside the COX-2 binding cavity (compare Tables 2 and 3).

3.5 Hydrophobicity of MMK16 Inside COX-2 and LOX-5

In order to investigate the role of hydrophobicity in binding, we have calculated the SASA of MMK16 inside the two protein cavities. Histograms of SASA values for the two systems are presented in Figure 12. MMK16 inside COX-2 appears to have almost two times greater water-accessible area (as expressed by a broader distribution, average 23.4 Å^2) than inside LOX-5 (average 13.0 Å^2). The increased hydrophobicity of MMK16 inside LOX-5 may additionally contribute to the better binding affinity for MMK16 inside COX-2.

3.6 Investigation of MMK16 Binding with STD NMR Experiments

Binding of compound MMK16 to LOX-3 was investigated using saturation transfer difference (STD) experiments.

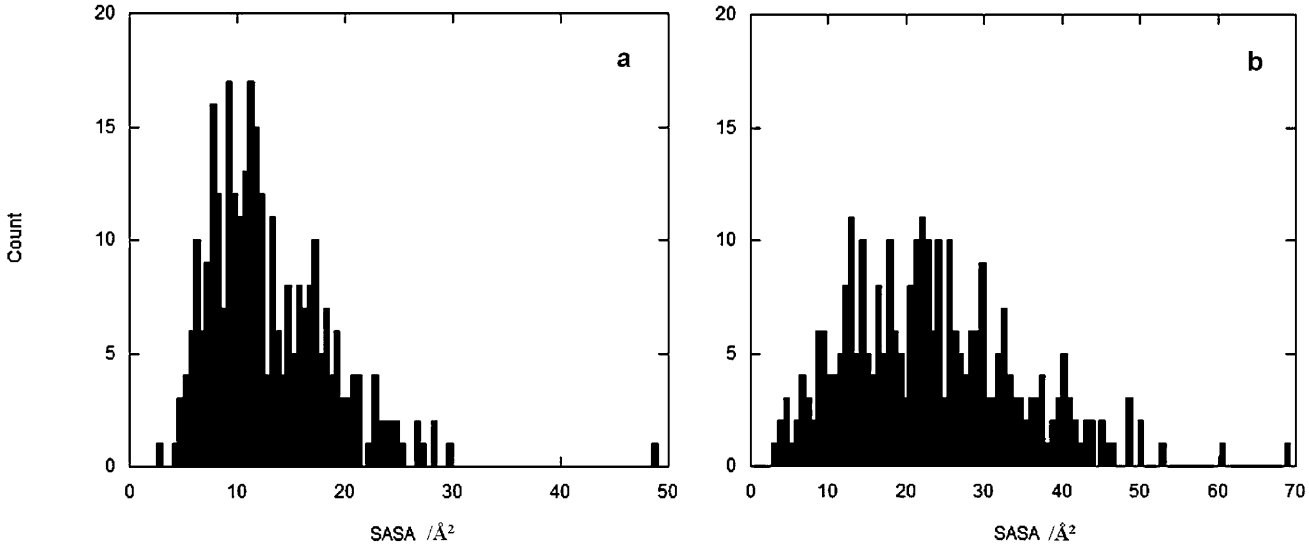

Figure 12. SASA histograms for MMK16 inside a) LOX-5, and b) COX-2.

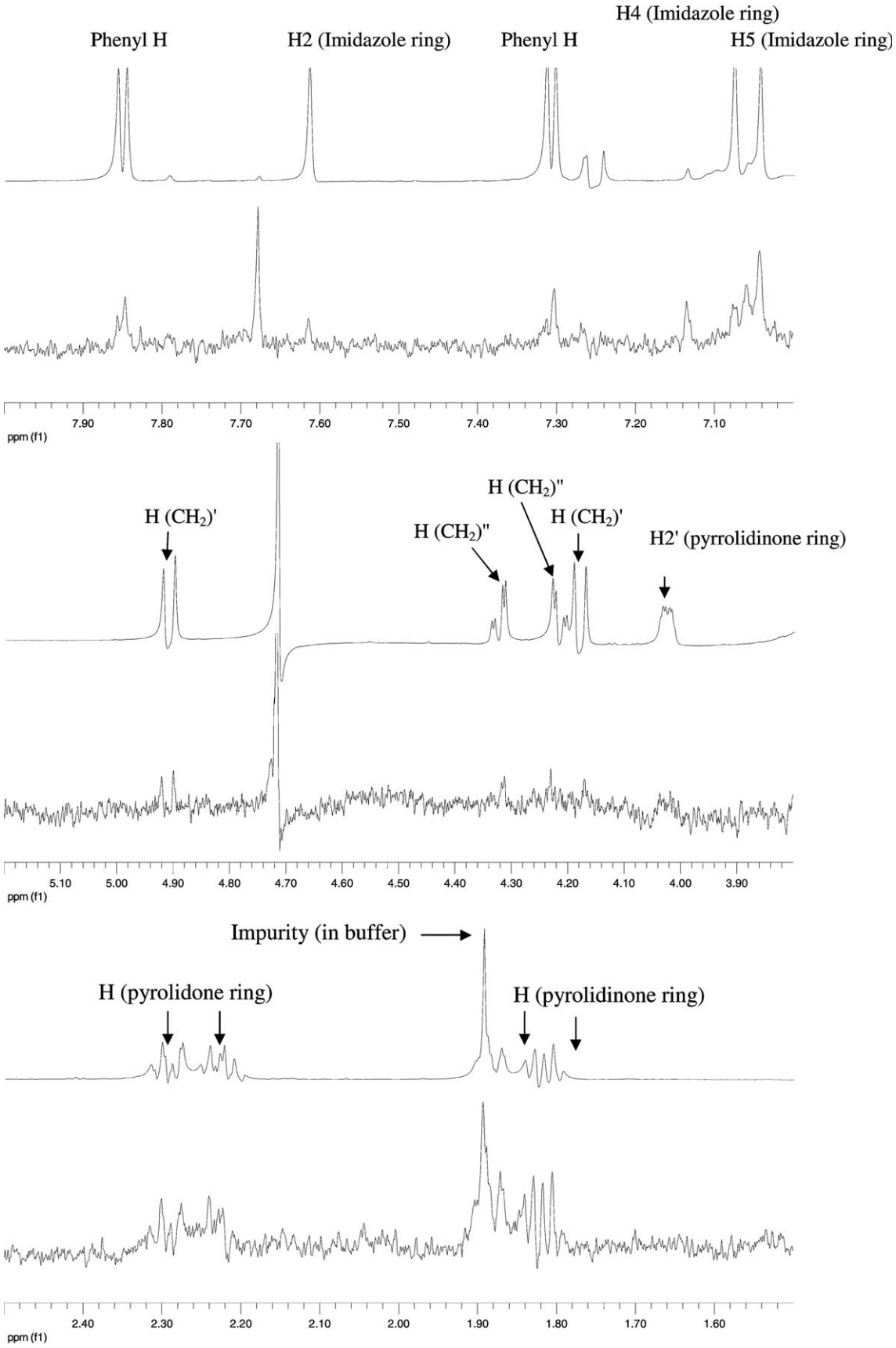

Figure 13. STD spectrum (bottom of various spectra regions) and reference spectrum (top of the various spectra regions) for the MMKI6 + caffeic acid + protein (MMK16 ratio 100 : 1). Note: Due to poor solubility of caffeic acid its ligand:protein ratio is approximately 20 : 1.

There were no MMK16 signals present in STD spectrum. This indicated that the binding regime of the compound MMK16 is not appropriate for STD experiments. Possible is that the compound binds either too strongly or it does not bind at all. To clarify this situation we have decided to perform a competition STD NMR experiment.[52] As mentioned above, caffeic acid is a known inhibitor of LOX-3 enzyme. In principle, STD signals of reporter ligand (caffeic acid in this case) should have reduced intensity when a strong binding competing ligand is added to the solution. Unfortunately, STD signals of caffeic acid recorded with the protein were very weak because of poor solubility of caffeic acid and were not appropriate for measuring intensity changes. However, when both compounds MMK16 and caffeic acid were recorded, the signals of compound MMK16 appeared in STD spectrum. This most probably indicates that due to competition between the two ligands, MMK16 binds with lower affinity and therefore falls into binding regime when STD signals can be observed. Less likely is that caffeic acid somehow promoted binding of compound MMK16 (Figure 13).

4 Conclusions

All docking results of MMK16 into the active site of cyclooxygenase suggest that MMK16 might inhibit the entrance of the substrate arachidonic acid into the binding cavity. This is due to its adopted orientation and the stabilization through electrostatic interactions inside the protein.

Docking and NMR binding results of MMK16 and caffeic acid into the active site of soybean Lipoxygenase-3 propose the competitive action between the two molecules at the active site without excluding a possible synergistic mechanism.

All members of lipoxygenase superfamily share an overall folding pattern and contain very similar non-heme iron binding sites. This is of a special interest in the present study, as an effort has been undertaken to predict the possible inhibitory activity of MMK16 at LOX-5 enzyme. The results of Table 1 (XP Gscore, $-\log K_d$) showed that the binding of MMK16 is favored in contrast to known inhibitor caffeic acid at the active site of LOX-5. The orientation of MMK16 at the active site is very important as the imidazole ring interacts electrostatically with Fe(III). MMK16 occupies the position of substrate aracidonic acid and is further stabilized through van der Waals and hydrogen bonding interactions inside the cavity.

The observations through docking, accompanied with MD as well as NMR binding studies suggest that the anti-inflammatory activity of MMK16 may be based on the inhibition of LOX-5/COX-2 enzymes.

Molecular dynamics simulation for the MMK16–COX-2 complex provided further insights into the binding modes of the protein. After the initial deviation from the docked system, the structure was eventually stabilized in a new conformation, determined primarily by the behavior of the membrane-binding domain and active site residues. Although it presented a very low degree of flexibility, the active site region underwent a structural rearrangement to account for more favorable interactions with MMK16 (namely with Arg120 and Ser530). MD results were complementary with those observed with docking ones because they showed that interactions of MMK16 with Tyr385 were unstable. A modified hydrogen bond network between MMK16 and COX-2 brought the complex to a stable state. Furthermore, an MD simulation was performed for MMK16 bound to LOX-5 to observe a similar, rapid structural change. A rearrangement of the MMK16-involved hydrogen bonds was also the reason for such a behavior. However, the remarkable stability of the active site residues throughout the simulation implied that they do not participate in any interactions with the substrate. A combination of hydrogen bonding interactions between MMK16 and (non-active site) residues 364, 426 and 601, eventually allowed the system to converge. Nevertheless, an electrostatic interaction with iron keeps MMK16 relatively near the active site (Fe-MMK16 distance ≈ 2 Å). Finally, an attempt to explain the finding that MMK16 presents higher binding affinity inside COX-2 than inside LOX-5 is offered, after evaluating the hydrogen bond patterns and the hydrophobic environment around MMK16: The greater number and occurrence of hydrogen bonds in COX-2 complex, along with the decreased hydrophobicity of the environment of MMK16 inside COX-2 may play significant role in the higher binding effect of COX-2 system.

Acknowledgement

Prof. T. Mavromoustakos acknowledges EAST NMR program for giving him the opportunity to run the NMR binding experiments. G. Leonis acknowledges the European Commission for the FP7-REGPOT-2009-1 Project 'ARCADE' (Grant Agreement No. 245866).

References

[1] D. A. Six, E. A. Dennis, *Biochim. Biophys. Acta* **2000**, *1488*, 1–19.
[2] W. L. Smith, D. L. DeW itt, R. M. Garavito, *Annu. Rev. Biochem.* **2000**, *69*, 145–182.
[3] W. L. Smith, D. L. Dewitt, *Adv. Immunol.* **1996**, *62*, 167–215.
[4] I. Morita, *Prostaglandins & Other Lipid Mediators* **2002**, *68–69*, 165–175.
[5] R. G. Kurumbail, A. M. Stevens, J. K. Gierse, J. J. McDonald, R. A. Stegeman, J. Y. Park, D. Glidehaus, J. M. Miyashiro, T. D. Penning, K. Seibert, *Nature* **1996**, *384*, 644–648.
[6] J. Y. Jouzeau, B. Terlain, A. Abid, E. Nedelec, P. Netter, *Drugs* **1997**, *53*, 563–582.
[7] B. Samuelsson, *Am. J. Respir. Crit. Care Medicine* **2000**, *161*, (2 II), S2–S6.

[8] W. Schonfeld, B. Schluter, R. Hilger, W. Konig, *Immunology* **1988**, *65*, 529 – 536.
[9] S. L. Spector, *Ann. Allergy Asthma Immunol.* **1995**, *75*, 463 – 474.
[10] D. W. P. Hay, T. J. Torphy, B. J. Undem, *Trends Pharmacol. Sci.* **1995**, *16*, 304 – 309.
[11] H. Sheng, J. Shao, J. D. Morrow, R. D. Beauchamp, R. N. DuBois, *Cancer Res.* **1998**, *58*, 362 – 366.
[12] M. Cuendet, J. M. Pezzuto, *Drug Metabol. Drug Interact.* **2000**, *17*, 109 – 157.
[13] A. J. Dannenberg, K. Subbaramaiah, *Cancer Cell.* **2003**, *4*, 431 – 436.
[14] J. Matsoukas, J. Hondrelis, M. Keramida, T. Mavromoustakos, A. Makriyannis, R. Yamdagni, Q. Wu, G. Moore, *J. Biol. Chem.* **1994**, *269*, 5303 – 5312.
[15] E. Theodoropoulou, T. Mavromoustakos, D. Panagiotopoulos, J. Matsoukas, J. Smith, *Let. Pep. Sci.* **1996**, *3*, 209 – 216.
[16] T. Mavromoustakos, A. Kolocouris, M. Zervou, P. Roumelioti, J. Matsoukas, R. Weisemann, *J. Med. Chem.* **1999**, *42*, 1714 – 1722.
[17] J. M. Matsoukas, L. Polevaya, J. Ancas, T. Mavromoustakos, A. Kolocouris, P. Roumelioti, D. V. Vlahakos, R. Yamdagni, Q. Wu, G. J. Moore, *Bioorg. Med. Chem. Lett.* **2000**, *8*, 1 – 10.
[18] P. Roumelioti, T. Tselios, K. Alexopoulos, T. Mavromoustakos, A. Kolocouris, G. J. Moore, J. M. Matsoukas, *Bioorg. Med. Chem. Lett.* **2000**, *10*, 755 – 758.
[19] L. Polevaya, T. Mavromoustakos, P. Zoumpoulakis, S. G. Grdadolnik, P. Roumelioti, N. Giatas, I. Mutule, T. Keivish, D. Vlahakos, E. Iliodromitis, D. Kremastinos, *Bioorg. Med. Chem.* **2001**, *9*, 1639 – 1647.
[20] P. Zoumpoulakis, S. G. Grdadolnik, J. Matsoukas, T. Mavromoustakos, *J. Pharmaceut. Biomed. Anal.* **2002**, *28*, 125 – 135.
[21] P. Roumelioti, L. Polevaya, P. Zoumpoulakis, N. Giatas, T. Keivish, A. Haritonova, A. Zoga, D. Vlahakos, E. Iliodromitis, D. Kremastinos, S. G. Grdadolnik, T. Mavromoustakos, J. Matsoukas, *Bioorg. Med. Chem. Lett.* **2002**, *12*, 2627 – 2633.
[22] P. Zoumpoulakis, A. Zoga, P. Roumelioti, N. Giatas, S. G. Grdadolnik, E. Iliodromitis, D. Vlahakos, D. Kremastinos, J. Matsoukas, T. Mavromoustakos, *J. Pharm. Biomed. Anal.* **2003**, *31*, 833 – 844.
[23] M. A.C. Preto, A. M. Hermani, L. S. Maia, T. Mavromoustakos, M. J. Ramos, *J. Phys. Chem. B* **2005**, *109*, 17743 – 17751.
[24] P. Zoumpoulakis, A. Politi, S. G. Grdadolnik, J. Matsoukas, T. Mavromoustakos, *J. Pharmaceut. Biomed. Anal.* **2006**, *40*, 1097 – 1104.
[25] T. Mavromoustakos, P. Zoumpoulakis, I. Kyrikou, A. Zoga, E. Siapi, M. Zervou, I. Daliani, D. Dimitriou, A. Pitsas, C. Kamoutsis, P. Laggner, *Curr. Top. Med. Chem.* **2004**, *4*, 445 – 459.
[26] T. Mavromoustakos, M. Zervou, P. Zoumpoulakis, I. Kyrikou, N. P. Benetis, L. Polevaya, P. Roumelioti, N. Giatas, A. Zoga, P. Moutevelis Minakakis, A. Kolocouris, D. Vlahakos, S. G. Grdadolnik, J. Matsoukas, *Curr. Top. Med. Chem.* **2004**, *4*, 385 – 401.
[27] J. M. Matsoukas, G. Agelis, A. Wahhab, J. Hondrelis, D. Panagiotopoulos, R. Yamdagni, Q. Wu, T. Mavromoustakos, H. L.S. Maia, R. Ganter, G. J. Moore, *J. Med. Chem.* **1995**, *38*, 4660 – 4669.
[28] P. Moutevelis-Minakakis, M. Gianni, H. Stougiannou, P. Zoumpoulakis, A. Zoga, A. D. Vlahakos, E. Iliodromitis, T. Mavromoustakos, *Bioorg. Med. Chem. Lett.* **2003**, *13*, 1737 – 1740.
[29] T. Mavromoustakos, P. Moutevelis-Minakakis, C. G. Kokotos, P. Kontogianni, A. Politi, P. Zoumpoulakis, J. Findlay, A. Cox, A. Balmforth, A. Zoga, E. Iliodromitis, *Bioorg. Med. Chem.* **2006**, *14*, 4353 – 4360.
[30] W. Sneader, in *Drug Discovery: A History*, Wiley, Chichester, UK, **2005**, p. 68.
[31] M. G. Malkowski, S. L. Ginnell, W. L. Smith, R. M. Garavito, *Science* **2000**, *289*, 1933 – 1937.
[32] W. F. Van Gunsteren, H. J. C. Berendsen, *J. Mol. Biol.* **1984**, *176*, 559 – 564.
[33] W. F. Van Gunsteren, H. J. C. Berendsen, *Angew. Chem. Int. Ed.* **1990**, *29*, 992 – 1023.
[34] E. Skrzypczak-Jankun, A. R. Bross, R. T. Carroll, W. R. Dunham, M. O. Funk Jr. , *J. Am. Chem. Soc.* **2001**, *123*, 10814 – 10820.
[35] W. Welch, J. Ruppert, A. N. Jain, *Chem. Biol.* **1996**. *3*, 449 – 462.
[36] J. Ruppert, W. Welch, A. N. Jain, *Protein Sci.* **1997**, *6*, 524 – 533.
[37] A. N. Jain, *J. Comput.-Aided Mol. Des.* **1996**, *10*, 427 – 440.
[38] *Glide*, Version 5.0, User Manual, Schrödinger, LLC, New York, NY, **2008**.
[39] J. R. Kiefer, J. L. Pawlitz, K. T. Moreland, R. A. Stegeman, W. F. Hood, J. K. Gierse, A. M. Stevens, D. C. Goodwin, S. W. Rowlinson, L. J. Marnett, W. C. Stallings, R. G. Kurumbail, *Nature* **2000**, *405*, 97 – 101.
[40] R. G. Kurumbail, A. M. Stevens, J. K. Gierse, J. J. McDonald, R. A. Stegeman, J. Y. Pak, D. Gildehaus, J. M. Miyashiro, T. D. Penning, K. Seibert, P. C. Isakson, W. C. Stallings, *Nature* **1996**, *384*, 644 – 648.
[41] L. Du, Z. Zhang, X. Luo, K. Chen, X. Shen, H. Jiang, *J. Biochem.* **2006**, *139*, 715 – 723.
[42] *Schrödinger Suite 2009 Protein Preparation Wizard*; Epik version 2.0, Schrödinger, LLC, New York, NY, **2009**.
[43] D. A. Case, T. A. Darden, T. E. Cheatham, III, C. L. Simmerling, J. Wang, R. E. Duke, R. Luo, R. C. Walker, W. Zhang, K. M. Merz, B. Roberts, B. Wang, S. Hayik, A. Roitberg, G. Seabra, I. Kolossváry, K. F. Wong, F. Paesani, J. Vanicek, J. Liu, X. Wu, S. R. Brozell, T. Steinbrecher, H. Gohlke, Q. Cai, X. Ye, J. Wang, M.-J. Hsieh, G. Cui, D. R. Roe, D. H. Mathews, M. G. Seetin, C. Sagui, V. Babin, T. Luchko, S. Gusarov, A. Kovalenko, P. A. Kollman, *AMBER 11*, University of California, San Francisco, **2010**.
[44] D. A. Case, T. E. Cheatham, III, T. A. Darden, H. Gohlke, R. Luo, K. M. Merz, Jr., A. Onufriev, C. L. Simmerling, B. Wang, R. J. Woods, *J. Comp. Chem.* **2005**, *26*, 1668–1688.
[45] V. Hornak, R. Abel, A. Okur, B. Strockbine, A. Roitberg, C. Simmerling, *Proteins–Structure Function and Bioinformatics* **2006**, *65*, 712.
[46] J. M. Wang, R. M. Wolf, J. W. Caldwell, P. A. Kollman, D. A. Case, *J. Comp. Chem.* **2004**, *25*, 1157 – 1174.
[47] A. Jakalian, B. L. Bush, D. B. Jack, C. I. Bayly, *J. Comp. Chem.* **2000**, *21*, 132 – 146.
[48] G. D. Hawkins, C. J. Cramer, D. G. Truhlar, *J. Phys. Chem.* **1996**, *100*, 19824.
[49] J. P. Ryckaert, G. Ciccotti, H. J. C. Berendsen, *J. Comp. Phys.* **1977**, *23*, 327.
[50] J. A. Izaguirre, D. P. Catarello, J. M. Wozniak, R. D. Skeel, *J. Chem. Phys.* **2001**, *114*, 2090 – 2098.
[51] A. Shrake, J. A. Rupley, *J. Mol. Biol.* **1973**, *79*, 351 – 371.
[52] M. Mayer, B. Meyer, *J. Am. Chem. Soc.* **2001**, *123*, 6108 – 6117.
[53] T. L. Hwang, A. J. Shaka, *J. Magn. Reson. Ser. A* **1995**, *112*, 275 – 279.
[54] C. Dalvit, *J. Biomol. NMR* **1998**, *11*, 437 – 444.

Received: October 26, 2010
Accepted: February 14, 2011
Published online: May 5, 2011

